LIP HEIGHT EFFECT IN QUADRANGULAR STEEL CONTAINERS

Einar Kolstad*, Vidar Frette & Bjarne Christian Hagen
Western Norway University of Applied Science, Haugesund, Norway

ABSTRACT

The reduction in the mass loss rate as function of lip height is investigated through 90 experiments with hydrocarbon pool fires in quadrangular containers of size 10 cm, 20 cm, and 30 cm. The results show a reduction in mass loss rate of 30-55 percent for 7 cm initial lip height compared with pool fires with no initial lip height.

INTRODUCTION

In the 1950's and 60's Blinov and Khudiakov [1,2] studied pool fires for containers with diameters from 0.011 m to 22.9 m, and found the variation with pool diameter in the regression rate of the fuel. They also showed that the lip height (the distance from the rim of the container to the fuel surface) influences the mass loss rate ($\dot{m}$). Based on the results from Blinov and Khudiakov, Hottel [3], divided pool fires into three regions depending on the flame structure: The laminar region, for small pools with diameter less than 3 cm, the transient region, for intermediate sized pools with diameter between 3 cm and 100 cm, and the turbulent region with pool diameter larger than 100 cm.

Emmon studied pool fires, and discovered that for alcohols $\dot{m}$ decreases with increasing lip-heights, but the effect is the opposite if container heating is taken in to the equation[4]. Orloff and De Rise examined pools with lip heights less than one tenth of the diameter. They discovered a significant change in the flame shape for experiments with small lip-height compared with experiments with no lips[5]. Despite these studies, there is still a lack of knowledge regarding the effect of lip-height on pool fires[6, p. 2582].

THEORY

Mass loss rate per unit area ($\dot{m}''$) for the liquid fuel in a pool fire is given in Eq. (1)[7].

$$\dot{m}'' = \dot{m}''_{\infty}\left(1 - e^{-\kappa\beta D}\right) \tag{1}$$

Here, $\dot{m}''_{\infty}$ is the asymptotic mass loss rate as the pool diameter (D) becomes large. κ and β are the absorption coefficient and the mean beam length corrector, respectively. The absorption coefficient accounts for the fluids ability to absorb radiation. Both κ and β are difficult to calculate, or determine, through experiments, their product is, therefore, given in literature. D is the equivalent diameter, the diameter of a circular pool with the same area as the pool of interest. Eq. (1) is valid for pool fires with

* E-mail: einar.kolstad@hvl.no Phone: +47 991 61 276

diameter ≥ 20 cm.

This section presents the governing equations for heat transfer in pool fires. Eq. (2) gives an expression for $\dot{m}''$. Here $\dot{Q}_F''$ is the heat flux towards the fuel surface per area, $\dot{Q}_L''$ is heat flux from the fuel surface and upwards per area, and L_v is the latent heat of evaporation of the fuel.

$$\dot{m}'' = \frac{\dot{Q}_F'' - \dot{Q}_L''}{L_V} \tag{2}$$

Hottel[3] expressed $\dot{Q}_F''$ as shown in Eq.(3). Drysdale rewrote and explained which of the three heat-transfer mechanisms that dominates for different pool sizes[8]. For pool fires in the laminar region, the conductive component becomes large, as the diameter is small. For pool fires in the turbulent region, the radiative component becomes large, with conduction and convection negligible in comparison. The last parenthesis in the radiative term approaches one as D increase, and therefore the heat flux towards the fuel surface per area becomes independent of the diameter in this region. For pool fires in the transient region, all heat exchange mechanisms contribute.

$$\dot{Q}_F'' = \frac{\overbrace{k_1\left(T_F - T_L\right)}^{\text{Conduction}}}{D} + \overbrace{k_2\left(T_F - T_L\right)}^{\text{Convection}} + \overbrace{k_3\left(T_F{}^4 - T_L{}^4\right)\left(1 - e^{-k_4 D}\right)}^{\text{Radiation}} \tag{3}$$

In Eq. (3), the constant k_1 accounts for the conductive heat transfer between the pool and the surroundings through the container wall. k_2 is the coefficient for convective heat transfer from the flame/hot gas to the pool surface. The constant k_3 is a combination of the Stefan-Boltzmann constant and the view factor from the flame to the pool surface. The constant k_4 describe the opacity and contains a combination of mean beam length factor, and the emission coefficient, $k_4 = \kappa\beta$. The radiation term includes re-radiation from the fuel surface and upwards through the temperature of the fuel surface, T_L. T_F is the flame temperature. The energy production from a pool fire is given in Eq. (4).

$$\dot{Q} = \chi \cdot \dot{m}'' \cdot A \cdot \Delta H_C \tag{4}$$

Here, A is the area of the pool, ΔH_C is heat of combustion of the fuel, and χ is the burning effectivity. The burning effectivity for heptane is about 0.7, the reminding energy is lost due to sot formation, residues and unburned fuel[7].

Figure 1 shows the energy flow in a pool fire. In Figure 1, quantities A-D are energy losses from the system, and E-I are internal energy exchange. A is radiation and convective heat losses from the flame to the surroundings. B, C, and D are convective heat losses from the upper part of the container, and from regions with gas, heptane, and water respectively. Energy absorbed by fluids is used to heat and evaporate liquid fuel and water. Referring to Eq. (3) E is radiation from the flame towards the fuel surface, and also accounts for re-radiation from the fuel surface. F is convective heating of the fuel surface from the hot gas between the flame and the fuel surface. G and H are conduction from the container wall to liquid fuel and water, respectively. I is heat exchange between heptane and water.

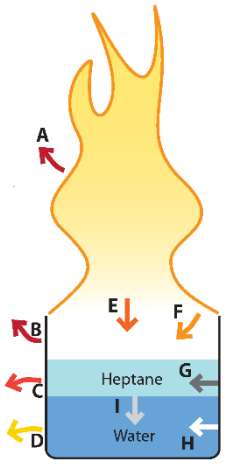

Figure 1: Heat exchange for a container with a pool fire. All symbols represent heat flows. A-D are the heat losses from the system, the others are internal heat exchanges. See further explanation in the main text.

EXPERIMENTAL SET-UP AND PROCEDURE

Steel containers are commonly used in fire experiments due to their fire resistance, availability, and price. Pool fires in the transient region have diameters from 3 cm to 100 cm. To examine pool fires in this region, quadrangular containers with size of 10 cm, 20 cm, and 30 cm were chosen (wall thickness 1 mm, and the container height was 10 cm for all container sizes), see Table 1. Experiments with three container sizes and three values for initial lip height have been carried out, leading to 9 experimental series, as shown in Table 1. Each series consisted of 10 repetitions, thus, the results reported below are based on 90 experiments. A 1 cm layer of heptane, on top of water was used in experiments with zero and 7 cm lip height. In 9 cm-lip-height experiments, water was not used. The range in the initial heptane mass given in Table 1 includes the lowest and highest initial mass used in the experiments. The initial mass varied in all series. The procedure for heptane filling was changed during this work. During the first part of the experiments a ruler was used to measure heptane level, later the amount of heptane to be used was determined through weighing. The latter method is more accurate (has better repeatability). Still a statistic analysis showed that there was no significant difference in the $\dot{m}''$ between these two procedures.

Table 1: Experimental overview.

Name	*Container size* [cm]	*Container mass* [g]	*Lip-height* [cm] *(Initial heptane mass* [g]*)*		
S10	10	399	0 (57-86)	7 (65-70)	9 (65-68)
S20	20	934	0 (332-452)	7 (332-342)	9 (330-346)
S30	30	1636	0 (765-858)	7 (840-1086)	9 (844-884)

In the first set of experiments, the lip height was set to zero, since Eq. (1) assumes no lip. 7 cm initial lip height was chosen to obtain a significant difference compared with the no lip scenario, but still with

water in the container. 9 cm initial lip height was chosen to obtain the largest possible difference in lip height compared with the no lip scenario. Figure 2 shows sketches of containers with water and heptane for the three different lip heights explored. The chosen water height imposes the desired lip height, h_{lip}. Note that in Figure 2c there is no water. The height of the heptane layer, $h_{C_7H_{16}}$, was the same in all

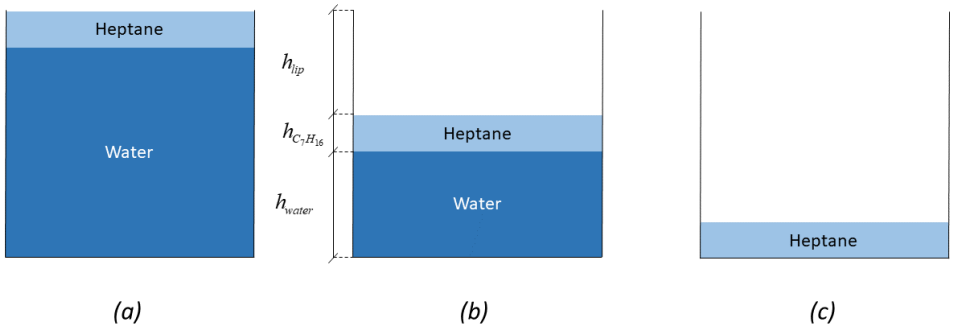

Figure 2: The three initial states considered in this paper. (a) A container flushed with heptane and water. (b) a container with water, heptane, and 7 cm lip height. (c) A container with 9 cm lip height and heptane, in this case water was not used.

experiments (within experimental variations see Table 1)

Figure 3 shows the experimental set up, with the filled container on top of a scale. The scale had a maximum capacity of 30 kg and a resolution of 0.1 g. An insulation block protected the scale from the heat. The red dots mark the positions of thermocouples used to monitor the temperature evolution.

The scale was placed on the table, and levelled. An insulation block was placed on the scale for thermal insulation between the scale and the container. The container was put on top of the insulation block at its centre, and water was filled to the required height. The water level was measured with a ruler. After filling in water, the scale was reset. Heptane was filled to the required level.

The data logger was started, heptane was ignited 5-10 s later, and a stopwatch started simultaneously. When the flame had extinguished, the stopwatch was halted, the data logging was turned off 5-10 s after the stopwatch.

It is important that the container is allowed to cool sufficiently before a new experiment is conducted. The water also has to be changed between each experiment, even if the water has cooled to ambient

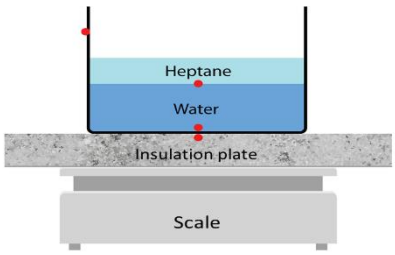

Figure 3: Scale with an insulation block, and the quadrangular container. The container either contains water and heptane, or only heptane, see Figure 2.

temperature. The water has to be changed because of residues from heptane in the water. Proper cleaning of the container between experiments is important. During a hydrocarbon fire a hydrophobic soot layer is formed on the inner side of the container, cleaning is therefore important.

The flame has a tendency to tilt towards one side; the airflows within the laboratory induce this flame tilting. This affect the radiation towards the fuel surface, moving the radiating flame away from the pool centre decreasing the radiation towards the fuel surface. The tilting was periodical and most of the time it was not present. Measurement of humidity during the experiments was not conducted. The temperature in the laboratory was between 13 °C and 18 °C.

RESULTS

Mass and temperature were measured as described in the previous section. Figure 4(a) shows a representative example of mass as function of time. The curve is slightly s-shaped as a result of fire growth and decay. Figure 4(b) and (c) show temperatures at the intersection between water and heptane, and between the container and the insulation block, and $\dot{m}''$ as functions of time. Figure 4(d) shows the temperature at the initial position of the heptane surface, and between the pan and insulation block. The $\dot{m}''$ curves show growth, steady burning, and decay phase. During the growth phase $\dot{m}''$ increases. The growth phase starts at ignition and last to around 180 s. The growth phase is followed by the steady burning phase from 180 s to 660 s. During this phase $\dot{m}''$ do not change substantially. During the decay phase $\dot{m}''$ decreases. This phase starts at 660 s and last till 720 s, when the fire ends. To calculate the average mass loss rate per unit area ($\bar{\dot{m}}''$), the mid-point, where half the initial heptane mass is burned away, was determined. Then $\bar{\dot{m}}''$ from 60 s before to 60 s after the mid-point, was calculated (see Figure 4(a)).

The behaviour of flames in quadrangular containers display both similarities and dissimilarities as compared with flames in circular containers. A striking difference is higher flame density near the corners of the quadrangular container compared with the lateral edges, (see Figure 5a). This is probably due to a stronger upwards airflow over the lateral edges into the flame compared with the case for the corners. The draft in the laboratory will sometimes force the flames towards one of the edges (see Figure 5a).

In Figure 5b the flame is located very close to the fuel surface, this is the situation early in the growth phase and in the decay phase. In Figure 5(c), the flame is located a several millimetres above the rim, and several centimetres above the fuel surface. This variation in the location of the flame is not dependent on pool geometry and can be understood as following. When $\dot{m}$ becomes large, there is necessarily increased flow of evaporated fuel, and air is not able to enter the container. The flame is, therefore, lifted above the rim of the container and burns where fuel and air mixes. In Figure 4(d) the temperature above the fuel surface shows high temperature (around 600 °C) in the growth phase indicating that there is a flame present. In the steady burning phase, the temperature is around 200 °C indicating that there is no flame just above the fuel surface. In the decay phase, the temperature is increasing to 600 °C indicating that the flame once again is located just above the fuel surface.

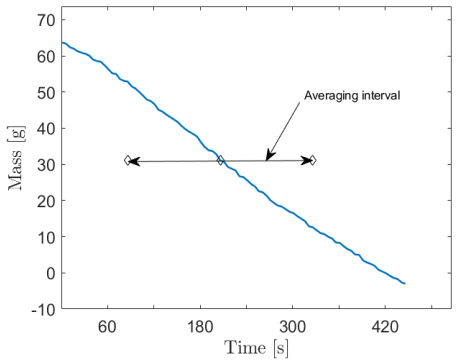

(a) S10, 0.5 cm mean lip height

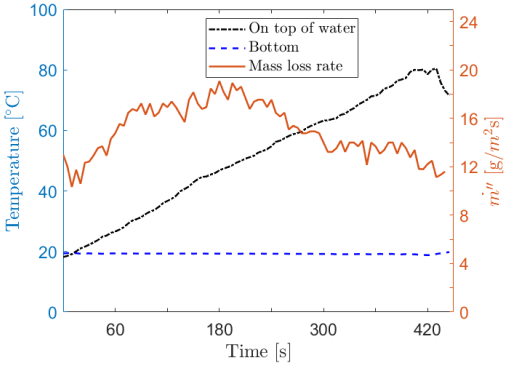

(b) S10, 0.5 cm mean lip height

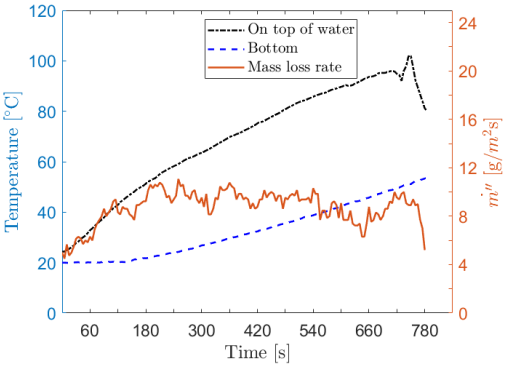

(c) S10, 7.5 cm mean lip height

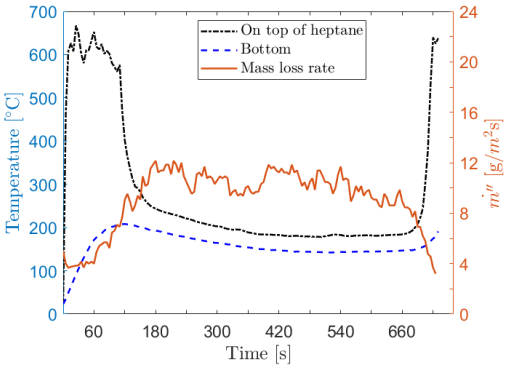

(d) S10, 9.5 cm mean lip height

Figure 4: Results from three S10 experiment, with 0.5 cm, 7.5 cm, and 9.5 cm mean lip height (average values during the experiments), (a) shows the mass as function of time, for 0.5 mean lip height. (b-d) shows the mass loss rate, the temperature at the bottom of the container, and temperature at the interface between water and heptane in parts (b) and (c) and just above the initial position of the heptane surface in part (d). Graph a and b is from the same experiment.

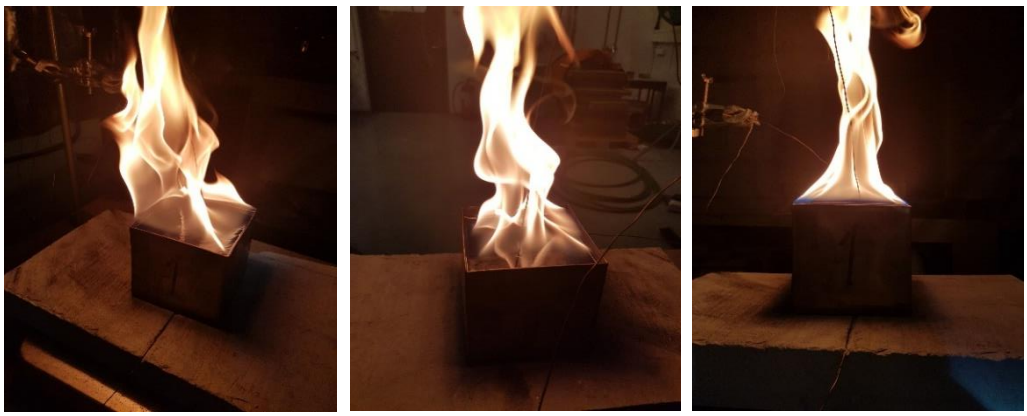

(a) *(b)* *(c)*

Figure 5: Photos showing characteristic features of the flame during the pool fires: (a) high flame density in corners, (b) flame burning near the fuel surface, (c) steady burning, and flames located several millimetre above the rim, and often several centimetres above the pool surface.

Figure 6 presents the average mass loss for each of the 90 experiments as a function of mean lip height (lip height averaged over each experiments). There are two important features. Firstly, there is large spread in values for $\bar{\dot{m}}''$ for S10 experiments with mean lip height 0.5 cm. Secondly most experiments with mean lip height of 9.5 cm has a higher $\bar{\dot{m}}''$ than those with 7.5 cm mean lip height. See discussion in later sections.

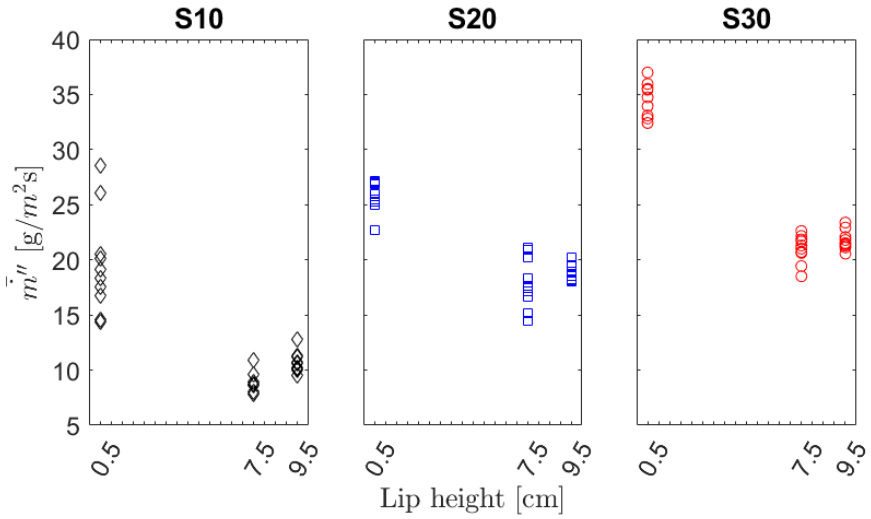

Figure 6: $\bar{\dot{m}}''$ for all 90 experiments, with $\bar{\dot{m}}''$ as function of lip height for each container size.

The average mass loss rate ($\tilde{\dot{m}}''$) for ten experiments ($\bar{\dot{m}}''$) for each container size (S10, S20 and S30) and lip height have been calculated together with the standard deviation, see Figure 7. The no-lip case has a higher $\tilde{\dot{m}}''$ than the 7, and 9 cm cases for all container sizes. The highest values for the standard deviation was found for S10, no initial lip height, and S20 with 7 cm initial lip height, with maximal value 15 percent of $\tilde{\dot{m}}''$.

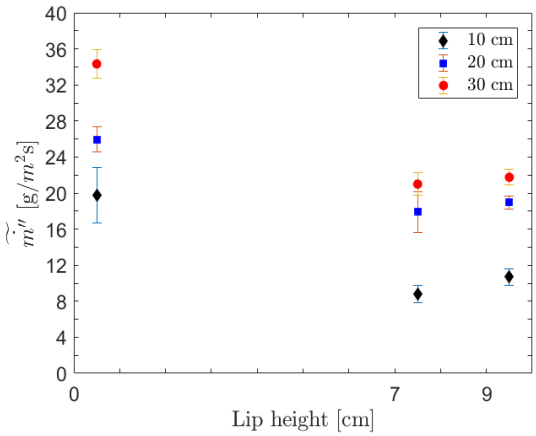

Figure 7: The average mass loss rate per unit area for 10 by 10, 20 by 20, and 30 by 30 cm containers, with lip heights of 0, 7, and 9 cm. There are 10 repetitions for all cases. Midsection method (see explanation in main text) is used to calculate $\tilde{\dot{m}}''$.

Figure 8 shows bottom temperature for three S10 experiments with no, 7 cm, and 9 cm initial lip height. The importance of water as heat sink in experiments with no, and 7 cm initial lip height is evident. The temperature at the container bottom is higher during the entire experiment for 9 cm lip height, than for 0 and 7 cm lip heights. Note in particular the rapid increase in temperature at the end of the 9 cm experiment. 0 and 7 cm lip experiments does not have such a rapid increase. The highest temperature for the no lip experiment is around 30 °C, for 7 cm lip height experiment it is 65 °C, but for 9 cm lip height the temperature becomes 200 °C.

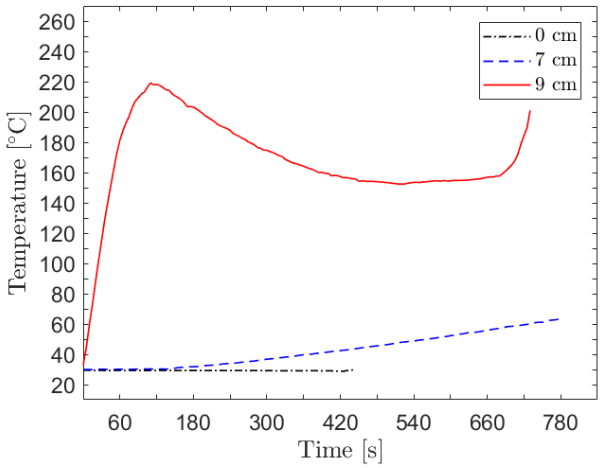

Figure 8: Temperature at the bottom of the container in S10 experiments with lip height of zero, 7 cm, and 9 cm. Data is taken from the same experiments as in Figure 4, with no averaging.

DISCUSSION

Mass loss rate in conjunction with heat release rate is one of the most important variables in fire experiments[9]. The current results show that lip height, water as heat sink, and area of the pan affects the mass loss rate.

There is a plain effect of lip height: As the lip-height increases from zero to 7 cm in a S10 container, $\tilde{\dot{m}}''$ decreases about 55 percent. For S20 and S30 the decrease in $\tilde{\dot{m}}''$ is 31 and 39 percent, respectively.

Water as heat sink is also important, as can be seen in the result from 7 cm and 9 cm lip height. $\tilde{\dot{m}}''$ for 9 cm lip height and no water is higher, than for 7 cm lip height. Water has nine times higher heat capacity than steel therefore water is a better heat sink than steel. In addition, the amount of water is higher than the amount of steel. Figure 8 shows how the bottom temperature develop during three S10 experiment with no lip, 7 cm lip height and 9 cm lip height. The temperature for 9 cm lip height reaches the boiling temperature to heptane (98 °C) after 200 s burning time. This is strikingly different from the cases with no lips where the temperature does not reach the boiling temperature of heptane, and 7 cm lip height that reaches the boiling temperature of heptane only 45 s before extinction. In short, the water layer efficiently keeps temperatures low for 0 cm and 7 cm lip-height experiments, while for 9 cm experiments a very hot container increases evaporation of heptane and lifts the 9 cm results in Figure 7 above the expected falling trend with increased lip height.

The standard deviations are small for all series, highest for S10 with no lip, where one standard deviation is 15 percent of $\tilde{\dot{m}}''$. Despite the uncertainties around start-mass, this indicates a good repeatability of

these experiments. There is high deviation in containers with no lip heights. This should be further investigated. It has been showed that even small lip heights influence the fire behaviour[5]. With such a susceptibility for small variations in initial conditions, the higher standard deviation for zero lip cases, than for the others is to be expected. It is reasonable to believe that for higher lips an extra millimetre would not change the outcome dramatically, the result from these experiments support such an assumptions.

Larger lip heights gives longer distances from the radiating flame to the evaporating fuel surface. Therefore, less radiation reaches the fuel bed, leading to lower $\dot{m}''$. Assuming the radiative flame volume is located 1 cm above the container edge, and the flame covers the same horizontal area as the container and the fuel surface, see Figure 5. If the fuel surface is located at the rim, the view factor becomes 0.8, but if the surface is located seven centimetre below the rim the view factor becomes 0.35. If the radiative energy is calculated, with flame temperature of 1200 °C, fuel temperature of 98 °C (boiling point of heptane), and an emissivity of 0.95 (equal to water), one finds 202 kW and 88 kW, respectively. Therefore, it is clear that the no lip scenarios receives more radiative energy than the 7 cm lip height scenario, and therefore, also more energy than the 9 cm lip height scenarios, which have an even lower view factor than the 7 cm lip height scenario.

Another approach is to calculate $\tilde{\dot{m}}''$ over the total duration of the experiment using all measuring point instead of the mid-part of the experiment, as for Figure 7. Figure 9 shows $\tilde{\dot{m}}''$ using an average of all measuring point in all experiments with same container size and initial lip height. Comparing Figure 7 and Figure 9, $\tilde{\dot{m}}''$ varies from 6 to 21 percent, and the results in Figure 9 give a lower $\tilde{\dot{m}}''$ than Figure 7 in all cases.

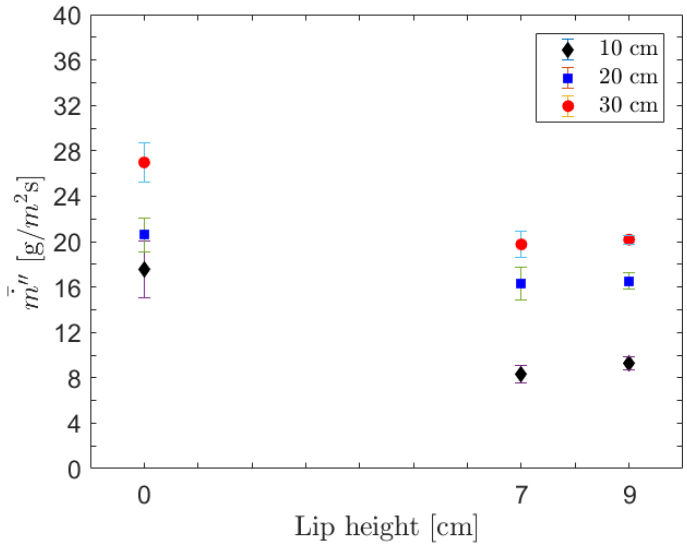

Figure 9: $\tilde{\dot{m}}''$ calculated over total burning time, see explanation in main text.

The $\tilde{\dot{m}}''$ values from Figure 7 could be compared with Eq. (1). Values $\dot{m}''_\infty = 101.0$ g/m²s and $k\beta = 1.1\ \mathrm{m}^{-1}$ have been used, these values are from literature [8] and does not depend on container size. For S10 one obtains $D = 0.113$ m. Notice that S10 is out of range for Eq. (1), which require that the diameter should be larger or equal to 20 centimetres. The S20 container have an equivalent diameter, $D = 0.226$ m, according to Eq. (1) this give $\dot{m}'' = 22.2\ \mathrm{g/m^2 s}$. In addition, S30 has $D = 0.339$ m,

which according to Eq. (1) gives $\dot{m}'' = 31.4$ g/m^{2}s. Comparing with the experiments for S10, S20, and S30 one has $\tilde{\dot{m}}''$ of 19.8, 26.0, and 34.3 g/m²s, respectively, when using the approach from Figure 7. If one use instead the overall burning time from Figure 9, one obtain $\tilde{\dot{m}}''$ is 17.5, 20.6 and 27.0 g/m²s, respectively. There is a good match between the equation and the experimental result but if a significant lip height are present, the estimations are less accurate. The experimental results for $\tilde{\dot{m}}''$ in S10, S20 and S30, with 7 cm initial lip height, are 8.8, 17.9 and 21.0 g/m²s, respectively, while the estimated mass loss are 34, 24, and 50 percent higher. The results from S10 can be ignored, since they are out of range for the equation, the result from S20 is acceptable in some senses, but for S30 the prediction is too high.

As expected, and shown in many previous experimental studies, the pool size is an important parameter for $\dot{m}''$, the S30 has higher $\tilde{\dot{m}}''$ compared with S10 and S20 for the same initial lip height. When comparing S30 with 7 cm lip height with S20 and S10 with no initial lip height, the S30, 7 cm lip height has almost the same $\tilde{\dot{m}}''$ as the S10 with no lip height and it is lower than for S20 with no lip height. Lip heights may therefore be as crucial for the $\tilde{\dot{m}}''$ as the container size.

CONCLUSION

The experiments has demonstrated that the mass loss rate ($\dot{m}$) not only is govern by the pool size, but also depends on the lip height.

From Figure 7 it is clear that $\dot{m}$ decreases with increasing lip height. The zero lip-height scenario is often assumed when calculating temperature, flame height, and smoke production. In most cases, however, consummation of fuel will induce a non-zero lip height situation, and thereby a lower $\dot{m}$. The decrease in $\dot{m}$ is significant and will lead to lower temperatures, and smoke production than calculations that assume a zero lip-height scenario.

This study investigated three lip heights using container with three different sizes. More extensive research is necessary to obtain systematic results for the lip heights influence on pool fires.

BIBLIOGRAFY

1. V. I. Blinov og G. N. Khudiakov, «Certain Laws Governing Diffusive Burning of Liquids,» 1957.
2. Blinov og Khudiakov, Diffusion Buring of Liquids, US army Translation, 1961.
3. H. C. Hottel, «Certain Laws Governing Diffusive Burning of Liquids,» Fire Research Abstracts and Reviews, pp. 41-44, September 1958.
4. H. W. Emmons, «Some Observetions on Pool Burning,» International Symposium on the Use of Models in Fire Research, pp. 50-67, July 1961.
5. L. Orloff og J. De Ris, «Froude Modeling of Pool Fires,» Nineteenth Symposium (international) on Combustion, The Combustion Institute, pp. 885-895, 1982.
6. SFPE, SFPE Handbook of Fire Protection Engineering, fifth editon, New York: Springer, 2016.
7. V. Babrauskas, «Estimating Large Pool Fire Burning Rates,» i Fire Technology 19, 1983, pp. 251-261.
8. D. Drysdale, An Introduction to fire dynamics, third edition, Wiley, 2011.
9. V. Babrauskas og R. D. Peacock, «Heat Release Rate: The Single Most Important Variable in Fire Hazard,» Fire Safety Journal 18, pp. 255-272, 1992.